Published in final edited form as:
Brain Struct Funct. 2014 January ; 219(1): . doi:10.1007/s00429-013-0508-8.

Differential regulation of parvalbumin and calretinin interneurons in the prefrontal cortex during adolescence

Adriana Caballero, **Eden Flores-Barrera**, **Daryn K. Cass**, and **Kuei Y. Tseng***
Department of Cellular and Molecular Pharmacology, The Chicago Medical School at Rosalind, Franklin University of Medicine and Science, North Chicago, IL 60064, USA

Abstract

Determining the normal developmental trajectory of individual GABAergic components in the prefrontal cortex (PFC) during the adolescent transition period is critical because local GABAergic interneurons are thought to play an important role in the functional maturation of cognitive control that occurs in this developmental window. Based on the expression of calcium-binding proteins, 3 distinctive subtypes of interneurons have been identified in the PFC: parvalbumin (PV)-, calretinin (CR)-, and calbindin (CB)-positive cells. Using biochemical and histochemical measures, we found that the protein level of PV is lowest in juveniles (postnatal day -PD- 25–35) and increases during adolescence (PD45–55) to levels similar to those observed in adulthood (PD65–75). In contrast, the protein expression of CR is reduced in adults compared to juvenile and adolescent animals, whereas CB levels remain mostly unchanged across the developmental window studied here. Semi-quantitative immunostaining analyses revealed that the periadolescent upregulation of PV and the loss of the CR signal appear to be attributable to changes in PV- and CR-positive innervation, which are dissociable from the trajectory of PV- and CR-positive cell number. At the synaptic level, our electrophysiological data revealed that a developmental facilitation of spontaneous glutamatergic synaptic inputs onto PV-positive/fast-spiking interneurons parallels the increase in prefrontal PV signal during the periadolescent transition. In contrast, no age-dependent changes in glutamatergic transmission were observed in PV-negative/non fast-spiking interneurons. Together, these findings emphasize that GABAergic inhibitory interneurons in the PFC undergo a dynamic, cell-type specific remodeling during adolescence and provide a developmental framework for understanding alterations in GABAergic circuits that occur in psychiatric disorders.

Keywords

interneurons; calcium-binding proteins; prefrontal cortex; fast-spiking; non-fast spiking

Introduction

The prefrontal cortex (PFC) belongs to a group of cortical regions that undergo major structural and functional remodeling during adolescence, a transitional period to adulthood during which a refinement of mature cognitive functions takes place (Casey et al. 2000; Spear 2000; Chambers et al. 2003; Crews et al. 2007). These include cognitive abilities such as working memory, decision-making, and increased inhibitory control, all of which are dependent on the maturation of the PFC (Best and Miller 2010; Luna et al. 2004). As one of the last cortical regions to develop (Huttenlocher 1990), it is not surprising that the

*Corresponding Author: Kuei Y. Tseng, MD, PhD, Department of Cellular and Molecular Pharmacology, The Chicago Medical School at RFUMS, 3333 Green Bay Rd, North Chicago, IL 60064, USA; kuei-yuan.tseng@rosalindfranklin.edu; Phone: 847-578-8655; Fax: 847-578-3268.

adolescent PFC network becomes highly susceptible to complex genetic-environmental factors (Andersen 2003). Hence, adolescence constitutes a vulnerable period during which altered prefrontal development can precipitate the onset of psychiatric disorders including schizophrenia, mood disorders, and drug abuse (Paus et al. 2008).

Among the several neurotransmitter systems undergoing postnatal maturation in the PFC, converging findings point towards a dysfunctional GABAergic circuit as a potential basis for the adolescent onset of cognitive deficits in schizophrenia (Hoftman and Lewis 2011; Benes and Berretta 2001; Uhlhaas and Singer 2011). Interestingly, studies from rodents and primates indicate that the local prefrontal GABAergic system experiences profound changes during adolescence (Benes et al. 1996; Vincent et al. 1995; Tseng and O'Donnell 2007; Kilb 2011). Such remodeling of local GABAergic interneurons is critical for the functional maturation of PFC network activity during the transition to adulthood (Tseng et al. 2009). However, it is not clear whether the prefrontal interneuronal deficits observed in schizophrenia result from a loss of GABAergic functionality during adulthood or rather a failure to mature into an adult GABAergic phenotype.

Early works have elegantly characterized the distribution, morphology, and abundance of local GABAergic interneuron populations in the PFC based on the expression of the calcium-binding proteins parvalbumin (PV), calretinin (CR), and calbindin (CB) (Conde et al. 1994; Gabbott and Bacon 1996; Gabbott et al. 1997a; Kubota and Kawaguchi 1994). Together, they account for more than 80% of the total GABAergic cells in the rat medial PFC (Gabbott et al. 1997a), highlighting the importance of specific calcium dynamics in interneuronal function. In addition to their role as calcium sensors (Eyles et al. 2002; Schwaller 2010), changes in the expression of calcium-binding proteins can define the functional characteristics of interneurons that impact the inhibitory control of prefrontal output. Such activity-dependent modulation of calcium-binding protein levels is best illustrated in PV-positive interneurons in which inhibition of glutamatergic transmission markedly reduces PV levels in cortical circuits (Behrens et al. 2007; Kinney et al. 2006). Thus, determining the normal trajectory of individual GABAergic components in the PFC during this developmental window could provide a framework to identify mechanisms underlying the onset of psychiatric disorders. In the present study, we employed biochemical and histochemical measures of calcium-binding proteins combined with electrophysiological recordings of synaptic activity to assess how PV-, CR- and CB-positive interneuronal function changes in the PFC during the periadolescent transition to adulthood.

Materials and Methods

Experimental age groups

All experimental procedures were conducted according to the USPHS Guide for the Care and Use of Laboratory Animals and approved by the Rosalind Franklin University Institutional Animal Care and Use Committee. Three age groups of male Sprague-Dawley rats (Harlan, Indianapolis, IN) from juveniles to young adults were compared in the present study: PD25–35, PD45–55, and PD65–75. Rats were group-housed (2–3 rats/cage) with food and water available *ad libitum*, and maintained at a constant temperature (21–23°C) and humidity in a 12 hour light-dark cycle. All animals were allowed to acclimate to the animal facility for at least 5 days before being used.

Detection of calcium-binding proteins by immunoblotting

All chemicals were obtained from Sigma-Aldrich (St. Louis, MO), except for β-mercaptoethanol (βME) that was purchased from Biorad (Hercules, CA), and paraformaldehyde (PFA) from Electron Microscopy Sciences (Hatfield, PA). Rats were

deeply anesthetized with 8% chloral hydrate (400 mg/kg, i.p.) and their brains quickly removed and blocked using an ice-cold steel brain matrix. Regions corresponding to the PFC indicated in the diagrams were harvested and lysed in cold lysis buffer (25 mM HEPES, 500 mM NaCl, 2 mM EDTA, 1 mM DTT, 0.1% NP-40) containing a cocktail of protease inhibitors (Thermo Scientific, Rockford, IL). Protein was quantified using the Biorad Dc Protein Assay according to manufacturer's instructions. Thirty micrograms of lysate per sample were resolved under reducing conditions by SDS-PAGE using Any kD™ pre-cast TGX Gels (BioRad, Hercules, CA). Proteins were then transferred to nitrocellulose membrane (Biorad), blocked with 5% Non-fat dry milk (Labscientific, Livingston, NJ) and immunoblotted using rabbit antibodies raised against PV (1:2,000), CR (1:5,000), and CB (1:5,000) (Swant, Bellinzona, Switzerland). Membranes were subsequently stripped in a solution of 62.5 mM Tris pH 6.8, 2% SDS, and 100 mM βME and re-probed with mouse anti-GADPH (1:10,000; Calbiochem/Millipore, Billerica, MA) as a loading control. All values were corrected for GAPDH loading and then normalized to the PD25–35 age group.

Immunohistochemical measures of calcium-binding proteins and cell counts

Rats were deeply anesthetized with 8% chloral hydrate (400 mg/kg i.p.) and transcardially perfused with 150 ml of cold saline followed by 150 ml of 4% PFA in phosphate buffered saline (0.1 M PBS). Brains were quickly removed, fixed in 4% PFA for 24 hrs, and stored in 30% sucrose in 0.1 M PBS for at least 3 days. Serial 50 μm-thick coronal sections were collected using a freezing stage (PFS-30MP controller, Physitemp Instruments, Clifton, NJ) on a sliding microtome (HM430, Thermo Scientific, FL). For each animal, three coronal sections that included the medial PFC located between bregma +3.2 and +2.5 mm (Paxinos and Watson 1998) were mounted on Superfrost Plus slides (VWR, Radnor, PA) and dried for 1 hr. Mounted sections were then incubated in 1% glycine in 0.1 M PBS for 1 hr (to quench potential autofluorescence), permeabilized, and blocked in 5% Normal Donkey Serum (NDS; Jackson Immunoresearch, Westgrove, PA) containing 1% BSA, 0.2% TX-100 in 0.1 M PBS for 1 hr. Subsequently, slides were incubated with rabbit antibodies against PV (1:2,000), CR (1:2,000), or CB (1:1,000) (Swant, Bellinzona, Switzerland) followed by donkey anti-rabbit IgG Alexa488-labeled antibody (1:500; Life Technologies, Grand Island, NY). After extensive washes in 0.1 M PBS, slides were mounted using Prolong Gold Anti-Fade reagent (Life Technologies, Eugene, OR). Slides were inspected using a Nikon E400 microscope with a 10X objective and images were captured with an ORCA-AG deep cooled digital camera (Hamamatsu, Bridgewater, NJ) under identical settings. Because of the small size of the medial PFC, two separate 1344×1024-pixel images covering approximately 90% of the prelimbic (PL) and infralimbic (IL) regions of the PFC were acquired for each coronal level examined. An additional image corresponding to the white matter (WM; forceps minor or anterior commissure) in the same section as the medial PFC was obtained from each coronal section for background correction. The mean fluorescence intensity (MFI) for each image (PL, IL, and WM) was measured using ImageJ (NIH, USA, http://rsb.info.nih.gov/ij/). For background correction, the corresponding WM value was subtracted from the MFI of PL and IL regions. The final MFI per animal was obtained by averaging the MFI of PL and IL from each rostro-caudal level. All tissue samples were processed in cohorts that contained juvenile animals (PD25–35) for normalization purposes. To determine the contribution of cell numbers to changes in MFI, the number of cells positive for PV and CR was estimated in the same 1344×1024-pixel images used to determine the mean fluorescence intensity across the 3 age groups. All cell counts were performed by an individual strictly blind to the experimental group.

Whole-cell patch clamp recordings of GABAergic interneurons in the PFC

As previously reported (Heng et al. 2011), rats were anesthetized with 8% chloral hydrate (400 mg/kg, i.p.) before decapitation. Brains were rapidly removed into ice-cold artificial

cerebrospinal fluid (aCSF) containing (in mM): 122.5 NaCl, 3.5 KCl, 25 $NaHCO_3$, 1.0 NaH_2PO_4, 0.5 $CaCl_2$, 3 $MgCl_2$, 20 glucose, 1.0 ascorbic acid (pH: 7.40–7.43, 295–305 mOsm). Coronal slices (300 μm-thick) containing IL and PL regions of the PFC were obtained using a Vibratome (Pelco 102, Ted Pella, Redding, CA) in ice-cold aCSF. Sections were then incubated at 33–35°C in aCSF under constant oxygenation with 95% O_2-5% CO_2 for at least 1 hr before recordings. In the recording aCSF, $CaCl_2$ was increased to 2.5 mM, $MgCl_2$ was decreased to 1 mM, and 10 μM picrotoxin was included to block GABA-A receptor-mediated transmission. Patch electrodes (5–8 MΩ) were obtained from 1.5 mm borosilicate glass capillaries (WPI, Sarasota, FL) with a horizontal puller (P-97, Sutter Instrument Co., Novata, CA). All recordings were conducted at 33–35 °C using a potassium-based internal solution containing 0.125% Neurobiotin and (in mM): 115 K-gluconate, 10 HEPES, 20 KCl, 2.0 $MgCl_2$, 2.0 Mg-ATP, 2.0 Na_2-ATP, 0.3 Na_2-GTP (pH 7.23–7.28, 280–282 mOsm). The recording aCSF was delivered to the recording chamber at the rate of ~2 ml/min.

Layer V interneurons in the IL/PL PFC were identified under visual guidance using infrared-differential interference contrast (IR-DIC) video microscopy with a 40X water-immersion objective (Olympus BX51-WI, Olympus America, Center Valley, PA). The image was detected with an IR-sensitive CCD camera (DAGE-MTI) and displayed on a monitor. Whole cell patch-clamp recordings were performed with MultiClamp 700B, digitized with Digidata 1440, and acquired with Axoscope 10.1 (Axon instruments/Molecular Devices, Sunnyvale, CA) at a sampling rate of 10 kHz. The liquid junction potential was not corrected and electrode potentials were adjusted to zero before obtaining the whole-cell configuration. Five minutes after obtaining the whole-cell configuration in current-clamp mode, somatic depolarizing and hyperpolarizing current pulses of 500 ms duration were applied to measure the neuronal excitability, the input resistance, afterhyperpolarization (AHP), and spike-frequency adaptation characteristic of the recorded cell. Recordings were then switched to voltage-clamp mode and held at −70 mV to measure spontaneous excitatory postsynaptic currents (EPSC). The mean frequency of spontaneous EPSC recorded in each neuron was estimated from at least 2 non-contiguous 60-second duration samples. Only neurons that remained stable for at least 20 min after obtaining the whole-cell configuration were included in the present study.

The morphology and location of recorded interneurons were determined by Neurobiotin staining. After completion of the recording session, the slices were fixed in 4% PFA in 0.1 M PBS at 4°C for approximately 12 hrs and stored in 0.1 M PBS until further processing. Staining was performed similarly to the immunohistochemical procedure described above, except that the tissue was blocked and permeabilized in 0.1 M PBS containing 5% NDS, 3% BSA and 2% TX-100. A subset of slices was incubated overnight at 4 °C with rabbit anti-PV. The following day slices were washed with 0.1 M PBS and incubated with Alexa488-labeled secondary antibody and Streptavidin-TRITC (1:500; Jackson Immunoresearch, West Grove, PA) for 3 hrs at room temperature. After extensive washes in PBS, slides were mounted and examined as described above.

Statistics

All data are expressed as mean ± SEM, and the statistical differences ($p<0.05$) among age groups were determined by one-way ANOVA using Statistica (StatSoft, Tulsa, OK). The Kolmogorov-Smirnov and Levene's tests were used to estimate the normality and homogeneity of variances, respectively. When ANOVAs were significant, the Tukey post-hoc test was applied to determine differences among experimental groups.

Results

Developmental changes of PV, CR, and CB protein levels in the PFC during the periadolescent transition as revealed by immunoblotting analyses

Two regions of the PFC (Fig. 1a) corresponding to the medial (infralimbic, prelimbic, cingulate) and dorsolateral (motor, somatosensory) regions were excised for immunoblotting analysis to determine whether the expression of PV, CR, and CB protein levels are developmentally regulated during the periadolescent period. We found that PV protein levels in the adolescent (PD45–55) and adult (PD65–75) medial PFC were similar and significantly higher (~36 and ~40%, respectively) than those of the juvenile (PD25–35) group, indicating that PV undergoes upregulation during the periadolescent transition to adulthood (Fig. 1a,b). A similar, yet more gradual increase in PV protein level was observed in the dorsolateral PFC where PV expression was significantly increased by 24% only in the lysates corresponding to adult animals (Fig. 1a,c). Conversely, CR protein levels in the PFC followed an opposite trajectory to that of PV such that CR expression in both regions of the PFC was highest in juveniles and lowest in adults (Fig. 2). Compared to juveniles, CR levels in the medial PFC were ~25% lower in adolescents and adults (Fig. 2a,b). In the dorsolateral PFC, there was no significant difference found between juveniles and adolescents; however, adults showed a 42% decrease in CR with respect to juveniles (Fig. 2a,c). CB protein levels in the PFC were also developmentally regulated during periadolescence, though the magnitude of such changes was markedly smaller when compared to those of PV and CR (Fig. 3). In particular, we were able to detect small but significant differences in prefrontal CB protein levels only between juvenile and adult animals. Relative to the juvenile group, the adult medial PFC exhibited a significant 13% increase in CB expression (Fig. 3a,b), whereas in the dorsolateral region CB levels decreased significantly by 9% (Fig. 3a,c). Together, our results indicate that immunoblotting is a highly sensitive method for quantifying and detecting differences in calcium-binding proteins in the PFC throughout closely defined developmental stages. These findings demonstrate for the first time that the three main markers of interneurons in the PFC undergo distinct developmental changes during the periadolescent transition.

Immunohistochemical detection of the distinct developmental trajectories of PV, CR, and CB protein expression in the PFC during the periadolescent transition

In order to visualize in detail the expression level of calcium-binding proteins in our region of interest, we processed brain sections from a second cohort of juvenile (PD25–35), adolescent (PD45–55), and adult (PD65–75) rats for semi-quantitative fluorescent immunohistochemistry of PV, CR, and CB in serial coronal sections of the medial PFC (see **Materials and Methods** for details).

As previously reported (Conde et al. 1994; Gabbott and Bacon 1996; Gabbott et al. 1997a), PV-positive cells and varicosities can be identified in all layers of the medial PFC with the exception of layer I. PV immunoreactivity in the medial PFC revealed a significant progressive augmentation in fluorescence intensity from juveniles to adolescents and adults (Fig. 4). More specifically, adolescents displayed an average increase in PV signal of 23% while adults showed a 58% increase, both relative to juveniles (Fig. 4a). Upon visual inspection of each section, we observed the increase in PV immunostaining was typically due to an increased PV signal in individual cells and processes. In this respect, it was observed that juvenile animals consistently showed a “punctate” profile in PV-positive processes, while both adolescents and adults displayed more widespread and higher intensity PV-positive processes across the medial PFC (Fig. 4b). We next determined if this age-dependent increase in prefrontal PV signal was due to an increase in the number of PV-positive cells. Cell counts from the same sections used to assess the mean PV fluorescence

signal showed a main effect of age with a small but significant increase in PV-positive cells only in the adult PFC relative to juveniles (Fig. 4c).

We also examined the pattern and trajectory of CR immunostaining in the medial PFC. Consistent with previous literature (Conde et al. 1994; Gabbott and Bacon 1996; Gabbott et al. 1997a; Gabbott et al. 1997b), CR staining typically revealed fusiform or bipolar cells with highly beaded dendrites whose somas mostly localized to superficial layers and whose dendrites extended vertically throughout the cortical layers (Fig. 5). Measures of CR fluorescence intensity showed a main effect of age with a significant downregulation of CR signal in adult animals compared to juveniles (Fig. 5a,b). There was a trend towards decreased CR staining in adolescents compared to juveniles which did not reach statistical significance. Visual inspection of the sections revealed that the loss of CR signal was commonly associated with decreased fluorescence in the neuropil area with no apparent change in cell numbers (Fig. 5b). Indeed, cell counts from the same sections utilized for mean fluorescence evaluation revealed no significant differences in CR-positive numbers in the three age groups analyzed here (Fig. 5c). Thus, these results suggest that the loss of CR signal in the medial PFC during the adolescent transition to adulthood is most likely due to a decrease in the distribution of CR-positive processes (i.e. dendrites), rather than a loss of CR-positive cells.

We also analyzed the trajectory of CB immunostaining in the medial PFC across the three age groups studied here (Fig. 6). CB immunofluorescence was detected prominently in layers II/III and CB-positive cells were detected across all layers, except layer I. Visual inspection of all medial PFC slices did not reveal any apparent differences in CB fluorescence or CB-positive cell numbers. Consistent with these observations, analysis of the mean CB fluorescent signal showed no statistically significant differences among juveniles, adolescents, and adults (Fig 6, lower panel), yet it displayed a similar trend as that observed by immunoblotting (Fig. 3). Similar to previous descriptions (Gabbott et al. 1997a; Kawaguchi and Kubota 1997), we observed a group of pyramidal cells in layers II/III weakly stained for CB. This feature made the differentiation of *bona fide* interneurons (with variable CB expression) from pyramidal cells extremely difficult and prevented us from unequivocally identifying and counting CB-positive interneurons within the medial PFC. Thus, the evidence presented here indicates that total CB levels remain relatively stable during the periadolescent transition to adulthood, but it cannot be excluded that this could reflect compensatory changes in the different populations of CB-positive cells (interneurons and pyramidal cells alike).

In summary, the immunostaining results substantiate the increased expression of PV and loss of CR signal observed by immunoblotting in the medial PFC during the periadolescent maturation. Importantly, such age-dependent effects appear to be attributable to changes in the extent and distribution of PV- and CR-positive processes in the medial PFC, which are relatively dissociable from the cell numbers.

Differential regulation of glutamatergic synaptic transmission onto fast-spiking (PV-positive) and non-fast spiking (PV-negative) interneurons in the medial PFC during the periadolescent transition

In other cortical structures, PV expression decreases upon afferent deprivation (Philpot et al. 1997; Carder et al. 1996), suggesting that the upregulation of PV signal observed in the medial PFC during the periadolescent transition could be associated with a facilitation of excitatory synaptic transmission onto PV-positive interneurons. To test this hypothesis, whole-cell patch-clamp recordings of interneuronal activity were performed in PFC brain slices from juvenile, adolescent, and adult groups described above.

All electrophysiological recordings were obtained from layer V medial PFC (prelimbic and infralimbic regions). We chose layer V because our previous study indicates that GABAergic interneurons in this layer are part of the neurobiological substrate that underlies the adolescent maturation of the medial PFC responses to dopamine modulation (Tseng and O'Donnell 2007). As shown before, medial PFC interneurons can be broadly categorized in two distinct groups, namely fast-spiking (FS) and non-fast spiking (NFS) interneurons (Fig. 7a,b) (Tseng and O'Donnell 2007; Tseng et al. 2008). Typically, FS interneurons exhibit a highly consistent PV expression and display a characteristic non-adapting firing pattern response to somatic current depolarization and prominent after-hyperpolarization potentials (AHP) (Fig. 7a; Table 1). In our present sample, all FS (n=18) and NFS (n=16) interneurons screened for PV immunolabeling were revealed as PV-positive and PV-negative, respectively (Fig. 7c,d).

Consistent with our previous report (Tseng and O'Donnell 2007), intrinsic neuronal properties of FS and NFS interneurons in the medial PFC remained relatively unchanged across the three age groups examined (Table 1). Only a small but significant main effect of age on membrane potential and AHP was found in FS interneurons. Relative to the juvenile PFC, FS interneurons from the PD65–75 age group exhibited a more hyperpolarized resting membrane potential and larger AHP amplitude (Table 1). At the synaptic level, we found that glutamatergic transmission onto FS interneurons undergoes a significant upregulation after PD35. We observed a highly significant increase in the number of spontaneous EPSC events in adolescents and adults compared to juveniles (Fig. 7e). Such age-dependent regulation of glutamatergic transmission was lacking in NFS interneurons (Fig. 7e). Notably, at any of the age periods studied here, NFS interneurons received a fraction of glutamatergic inputs compared to FS interneurons as revealed by the mean frequency of spontaneous EPSC in both interneuronal populations. In summary, our electrophysiological data show that the developmental gain of glutamatergic function onto prefrontal PV-positive/FS interneurons parallels the increase in PV signal observed in the PFC during the periadolescent transition.

Discussion

Using biochemical and histochemical measures, we have found that calcium-binding proteins PV and CR are differentially regulated in the PFC during the periadolescent transition period. PV expression is lowest in juveniles and is significantly increased in adolescents and young adults. In contrast, the expression of CR is reduced in adults and adolescents compared to juvenile animals, whereas the expression of CB remains mostly unchanged across the three age groups studied. Electrophysiological studies expand upon these findings suggesting that the increase in PV signal in the PFC is associated with an augmentation of glutamatergic transmission onto PV-positive/FS interneurons. Interestingly, such a developmental facilitation of glutamatergic control was lacking in PV-negative/NFS interneurons. Together, the present results emphasize the dynamic, cell-specific changes occurring in prefrontal interneurons during the periadolescent period and posit adolescence as a window of vulnerability for the maturation of GABAergic circuits.

PV-positive cells are the most abundant class of GABAergic interneurons in the rat PFC (Gabbott et al. 1997a). In the developmental window studied here, total PV levels increased more than 50% in the medial PFC of adults compared to juveniles, especially at the level of PV-positive processes, despite that the number of PV-positive cells only slightly increased. This developmental upregulation of PV signal could therefore be attributable to the functional maturation of PV interneurons that endures through adulthood, since the expression level of PV and the functional profile of PV-positive cells are tightly correlated (Behrens et al. 2007; Eggermann and Jonas 2011). Our electrophysiological data further

indicate that acquisition of mature PV levels during adolescence is associated with a facilitation of glutamatergic transmission onto PV-positive/FS interneurons. Although we cannot state conclusively that glutamatergic inputs upregulate the PV signal, it is likely that increased PV expression during adolescence is an activity-driven event at a time when metabolic demand is increased, as indicated by the specific enrichment of energy metabolism genes during adolescence (Harris et al. 2009). Accordingly, PV-positive interneurons show the highest amount of cytochrome C among adult cortical neurons, indicative of increased mitochondrial metabolism (Gulyas et al. 2006). Thus, upregulation of PV might be a widespread phenomenon in the brain, yet it may occur last in prefrontal regions consistent with the ontogeny of brain structures (Solbach and Celio 1991). This pattern is reiterated within the neocortex itself, with sensory cortices showing the first appearance of PV-positive cells at PD8–11, whereas associative cortices start displaying PV-positive cells by PD11–13 (Alcantara et al. 1993). In line with the hypothesis that adolescence constitutes a sensitive developmental period for other limbic structures, we recently found that a similar periadolescent regulation of PV-positive interneurons occurs in the ventral hippocampus (Caballero et al. 2012).

PV-positive cells in cortical circuits are often referred to as FS GABAergic interneurons and are functionally positioned to exert fast and timely feedforward inhibitory regulation of cortical output activity in response to synchronous glutamatergic drive (see review by (Bartos and Elgueta 2012)) In the PFC, such inhibitory control is critical for fine-tuning and spatial selectivity of pyramidal cell firing (Rao et al. 2000). Although the underlying mechanism for the periadolescent facilitation of glutamatergic synaptic transmission onto prefrontal FS interneurons remains to be determined, three major brain regions, in addition to intracortical inputs, are known to provide strong glutamatergic afferents to the PFC. These include the ventral hippocampus (Cenquizca and Swanson 2007; Jay and Witter 1991; Swanson 1981; Hoover and Vertes 2007), the amygdala (Conde et al. 1995; McDonald 1996) and the mediodorsal thalamus (Giguere and Goldman-Rakic 1988; Groenewegen 1988; Rotaru et al. 2005). Afferents originating from these regions are critical for amplifying PFC-dependent cognitive processes and integrating emotionally salient information (Ishikawa and Nakamura 2003; Sherwood et al. 2010) Thus, the increased glutamatergic drive onto FS interneurons during the periadolescent transition period is expected to enhance the gain of local prefrontal GABAergic function thought to be associated with the adolescent maturation of cognitive abilities including working memory, decision making and impulse control (O'Donnell 2011; Uhlhaas and Singer 2011).

In addition to displaying opposite developmental trajectories to that of PV, CR-positive cells arise much earlier in all regions of the brain compared to CB and PV (Andressen et al. 1993). In the rat medial PFC, CR-positive interneurons are less numerous when compared to PV-positive neurons (Gabbott et al. 1997a) and exhibit NFS electrophysiological characteristics with either an irregular-spiking (Ascoli et al. 2008), regular spiking, or burst spiking (Kawaguchi and Kubota 1997) pattern. CR-positive interneurons are known to innervate deep layer pyramidal cells as well as to form synaptic contacts with other GABAergic interneurons in layer III, including those in their own class (Gabbott et al. 1997a; Meskenaite 1997). In the medial PFC, baskets of CR-positive processes have been observed surrounding pyramidal neurons in layer V and GABAergic interneurons in layer III (Gabbott and Bacon 1996; Gabbott et al. 1997a). The latter makes them ideally positioned to exert inhibitory control over other interneurons in the PFC. Thus, it is tempting to speculate that a downregulation of CR expression allows the upregulation of PV-positive interneuronal function during the adolescent transition to adulthood. A switch from NFS to FS control of local prefrontal inhibition may be required for the maturation of PFC-dependent cognitive processes that occurs during adolescence.

Technical Limitations

CB-positive neurons constitute the most varied phenotypic group of interneurons in the cortex, frequently co-localizing with other peptides like somatostatin and neuropeptide Y, each with their own defined physiological properties (Kubota and Kawaguchi 1994; Ascoli et al. 2008). Our results showed a small but significant upregulation of total CB protein levels in adults compared to juveniles, a trend also observed at the level of CB immunohistochemistry. However, given the diversity of interneuronal subpopulations that express CB, we cannot discard the possibility that the relative stability of CB expression is caused by opposite compensatory changes in the different subpopulations of interneurons or even in layer II/III pyramidal cells, which express low levels of CB (Kubota and Kawaguchi 1994; Gabbott et al. 1997a). The characterization of the development of CB-positive subpopulations and their biological impact on local prefrontal GABAergic function remain to be investigated.

Finally, it is important to point out that all cell count data shown in the present study were aimed to determine the contribution of cell numbers to changes observed at the level of the mean fluorescence intensity (see details in Methods). Given that a systematic sampling of the PFC from a randomized starting point was not the method used here, the differential regulation in the number of PV- and CR-positive cells observed may not be representative of the PFC as a whole but only pertains to the samples analyzed. Thus, a detailed stereological assessment of PV-, CR-, and CB-positive interneuron numbers specifically during adolescence is warranted. In addition, it is acknowledged that in order to verify that the observed changes are a reflection of regulatory mechanisms operating in the adolescent brain (versus a mechanism that operates across the lifespan or as a function of cumulative experience), future studies would have to include a developmental period in which the changes reported here do not occur.

Functional Implications

Understanding the age-dependent trajectory of cortical activity with a focus on prefrontal interneuronal circuits is highly relevant to the pathophysiology of schizophrenia since PFC impairments in this disorder are associated with reduced gamma oscillations in EEG readouts, an effect thought to be due to a developmental attenuation of cortical inhibitory transmission (Uhlhaas and Singer 2010). Major alterations in prefrontal GABAergic interneurons in schizophrenia have been observed at the level of PV expression without changes in the total number of PV-positive cells (Woo et al. 1998). These include downregulation of PV levels and GAD67 mRNA (Volk et al. 2000; Hashimoto et al. 2003), suggesting that PV-positive interneuronal functionality is reduced in schizophrenia. In light of our present findings, prefrontal impairments in schizophrenia may arise from a lack of the normative PV upregulation during adolescence, rather than a loss of PV. The upregulation of PV expression is likely due to the rise of excitatory inputs, resulting in a fully mature GABAergic profile. Thus, failure to gain cortical GABAergic function during adolescence would result in prefrontal disinhibition and the emergence of PFC-dependent deficits such as those seen in schizophrenia. In conclusion, pre- and postnatal insults that arrest the functional maturation of PV-positive/FS GABAergic interneurons that occurs in the PFC during adolescence could cause long-lasting prefrontal deficits only revealed in late adolescence and early adulthood when local inhibitory control must match the normative increase in prefrontal excitatory drive (Heng et al. 2011; Tseng and O'Donnell 2005).

Acknowledgments

Supported by Rosalind Franklin University, the Brain Research Foundation (KYT) and the National Institutes of Health Grant R01-MH086507 (KYT). We thank Daniel Thomases for editorial assistance and helpful comments.

References

Alcantara S, Ferrer I, Soriano E. Postnatal development of parvalbumin and calbindin D28K immunoreactivities in the cerebral cortex of the rat. Anat Embryol (Berl). 1993; 188 (1):63–73. [PubMed: 8214625]

Andersen SL. Trajectories of brain development: point of vulnerability or window of opportunity? Neurosci Biobehav Rev. 2003; 27 (1–2):3–18. [PubMed: 12732219]

Andressen C, Blumcke I, Celio MR. Calcium-binding proteins: selective markers of nerve cells. Cell Tissue Res. 1993; 271 (2):181–208. [PubMed: 8453652]

Ascoli GA, Alonso-Nanclares L, Anderson SA, Barrionuevo G, Benavides-Piccione R, Burkhalter A, Buzsaki G, Cauli B, Defelipe J, Fairen A, Feldmeyer D, Fishell G, Fregnac Y, Freund TF, Gardner D, Gardner EP, Goldberg JH, Helmstaedter M, Hestrin S, Karube F, Kisvarday ZF, Lambolez B, Lewis DA, Marin O, Markram H, Munoz A, Packer A, Petersen CC, Rockland KS, Rossier J, Rudy B, Somogyi P, Staiger JF, Tamas G, Thomson AM, Toledo-Rodriguez M, Wang Y, West DC, Yuste R. Petilla terminology: nomenclature of features of GABAergic interneurons of the cerebral cortex. Nat Rev Neurosci. 2008; 9 (7):557–568. [PubMed: 18568015]

Bartos M, Elgueta C. Functional characteristics of parvalbumin- and cholecystokinin-expressing basket cells. J Physiol. 2012; 590 (Pt 4):669–681. [PubMed: 22250212]

Behrens MM, Ali SS, Dao DN, Lucero J, Shekhtman G, Quick KL, Dugan LL. Ketamine-induced loss of phenotype of fast-spiking interneurons is mediated by NADPH-oxidase. Science. 2007; 318 (5856):1645–1647. [PubMed: 18063801]

Benes FM, Berretta S. GABAergic interneurons: implications for understanding schizophrenia and bipolar disorder. Neuropsychopharmacology. 2001; 25 (1):1–27. [PubMed: 11377916]

Benes FM, Vincent SL, Molloy R, Khan Y. Increased interaction of dopamine-immunoreactive varicosities with GABA neurons of rat medial prefrontal cortex occurs during the postweanling period. Synapse. 1996; 23 (4):237–245. [PubMed: 8855508]

Best JR, Miller PH. A developmental perspective on executive function. Child Dev. 2010; 81 (6): 1641–1660. [PubMed: 21077853]

Caballero, A.; Cass, DK.; Tseng, KY. Society for Neuroscience. Vol. 736. New Orleans, LA: Society for Neuroscience Online; 2012. Developmental trajectories of parvalbumin and calretinin positive interneurons in the prefrontal cortex and ventral hippocampus during adolescence; p. 708/A765

Carder RK, Leclerc SS, Hendry SH. Regulation of calcium-binding protein immunoreactivity in GABA neurons of macaque primary visual cortex. Cereb Cortex. 1996; 6 (2):271–287. [PubMed: 8670656]

Casey BJ, Giedd JN, Thomas KM. Structural and functional brain development and its relation to cognitive development. Biol Psychol. 2000; 54 (1–3):241–257. [PubMed: 11035225]

Cenquizca LA, Swanson LW. Spatial organization of direct hippocampal field CA1 axonal projections to the rest of the cerebral cortex. Brain Res Rev. 2007; 56 (1):1–26. [PubMed: 17559940]

Chambers RA, Taylor JR, Potenza MN. Developmental neurocircuitry of motivation in adolescence: a critical period of addiction vulnerability. Am J Psychiatry. 2003; 160 (6):1041–1052. [PubMed: 12777258]

Conde F, Lund JS, Jacobowitz DM, Baimbridge KG, Lewis DA. Local circuit neurons immunoreactive for calretinin, calbindin D-28k or parvalbumin in monkey prefrontal cortex: distribution and morphology. J Comp Neurol. 1994; 341 (1):95–116. [PubMed: 8006226]

Conde F, Maire-Lepoivre E, Audinat E, Crepel F. Afferent connections of the medial frontal cortex of the rat. II. Cortical and subcortical afferents. J Comp Neurol. 1995; 352 (4):567–593. [PubMed: 7722001]

Crews F, He J, Hodge C. Adolescent cortical development: a critical period of vulnerability for addiction. Pharmacol Biochem Behav. 2007; 86 (2):189–199. [PubMed: 17222895]

Eggermann E, Jonas P. How the ‘slow’ Ca(2+) buffer parvalbumin affects transmitter release in nanodomain-coupling regimes. Nat Neurosci. 2011; 15 (1):20–22. [PubMed: 22138646]

Eyles DW, McGrath JJ, Reynolds GP. Neuronal calcium-binding proteins and schizophrenia. Schizophr Res. 2002; 57 (1):27–34. [PubMed: 12165373]

Gabbott PL, Bacon SJ. Local circuit neurons in the medial prefrontal cortex (areas 24a,b,c, 25 and 32) in the monkey: I. Cell morphology and morphometrics. J Comp Neurol. 1996; 364 (4):567–608. [PubMed: 8821449]

Gabbott PL, Dickie BG, Vaid RR, Headlam AJ, Bacon SJ. Local-circuit neurones in the medial prefrontal cortex (areas 25, 32 and 24b) in the rat: morphology and quantitative distribution. J Comp Neurol. 1997a; 377 (4):465–499. [PubMed: 9007187]

Gabbott PL, Jays PR, Bacon SJ. Calretinin neurons in human medial prefrontal cortex (areas 24a,b,c, 32', and 25). J Comp Neurol. 1997b; 381 (4):389–410. [PubMed: 9136798]

Giguere M, Goldman-Rakic PS. Mediodorsal nucleus: areal, laminar, and tangential distribution of afferents and efferents in the frontal lobe of rhesus monkeys. J Comp Neurol. 1988; 277 (2):195–213. [PubMed: 2466057]

Groenewegen HJ. Organization of the afferent connections of the mediodorsal thalamic nucleus in the rat, related to the mediodorsal-prefrontal topography. Neuroscience. 1988; 24 (2):379–431. [PubMed: 2452377]

Gulyas AI, Buzsaki G, Freund TF, Hirase H. Populations of hippocampal inhibitory neurons express different levels of cytochrome c. Eur J Neurosci. 2006; 23 (10):2581–2594. [PubMed: 16817861]

Harris LW, Lockstone HE, Khaitovich P, Weickert CS, Webster MJ, Bahn S. Gene expression in the prefrontal cortex during adolescence: implications for the onset of schizophrenia. BMC Med Genomics. 2009; 2:28. [PubMed: 19457239]

Hashimoto T, Volk DW, Eggan SM, Mirnics K, Pierri JN, Sun Z, Sampson AR, Lewis DA. Gene expression deficits in a subclass of GABA neurons in the prefrontal cortex of subjects with schizophrenia. J Neurosci. 2003; 23 (15):6315–6326. [PubMed: 12867516]

Heng LJ, Markham JA, Hu XT, Tseng KY. Concurrent upregulation of postsynaptic L-type Ca(2+) channel function and protein kinase A signaling is required for the periadolescent facilitation of Ca(2+) plateau potentials and dopamine D1 receptor modulation in the prefrontal cortex. Neuropharmacology. 2011; 60 (6):953–962. [PubMed: 21288471]

Hoftman GD, Lewis DA. Postnatal developmental trajectories of neural circuits in the primate prefrontal cortex: identifying sensitive periods for vulnerability to schizophrenia. Schizophr Bull. 2011; 37 (3):493–503. [PubMed: 21505116]

Hoover WB, Vertes RP. Anatomical analysis of afferent projections to the medial prefrontal cortex in the rat. Brain Struct Funct. 2007; 212 (2):149–179. [PubMed: 17717690]

Huttenlocher PR. Morphometric study of human cerebral cortex development. Neuropsychologia. 1990; 28 (6):517–527. [PubMed: 2203993]

Ishikawa A, Nakamura S. Convergence and interaction of hippocampal and amygdalar projections within the prefrontal cortex in the rat. J Neurosci. 2003; 23 (31):9987–9995. [PubMed: 14602812]

Jay TM, Witter MP. Distribution of hippocampal CA1 and subicular efferents in the prefrontal cortex of the rat studied by means of anterograde transport of Phaseolus vulgaris-leucoagglutinin. J Comp Neurol. 1991; 313 (4):574–586. [PubMed: 1783682]

Kawaguchi Y, Kubota Y. GABAergic cell subtypes and their synaptic connections in rat frontal cortex. Cereb Cortex. 1997; 7 (6):476–486. [PubMed: 9276173]

Kilb W. Development of the GABAergic System from Birth to Adolescence. Neuroscientist. 2011

Kinney JW, Davis CN, Tabarean I, Conti B, Bartfai T, Behrens MM. A specific role for NR2A-containing NMDA receptors in the maintenance of parvalbumin and GAD67 immunoreactivity in cultured interneurons. J Neurosci. 2006; 26 (5):1604–1615. [PubMed: 16452684]

Kubota Y, Kawaguchi Y. Three classes of GABAergic interneurons in neocortex and neostriatum. Jpn J Physiol. 1994; 44(Suppl 2):S145–148. [PubMed: 7538606]

Luna B, Garver KE, Urban TA, Lazar NA, Sweeney JA. Maturation of cognitive processes from late childhood to adulthood. Child Dev. 2004; 75 (5):1357–1372. [PubMed: 15369519]

McDonald AJ. Glutamate and aspartate immunoreactive neurons of the rat basolateral amygdala: colocalization of excitatory amino acids and projections to the limbic circuit. J Comp Neurol. 1996; 365 (3):367–379. [PubMed: 8822176]

Meskenaite V. Calretinin-immunoreactive local circuit neurons in area 17 of the cynomolgus monkey, Macaca fascicularis. J Comp Neurol. 1997; 379 (1):113–132. [PubMed: 9057116]

O'Donnell P. Adolescent onset of cortical disinhibition in schizophrenia: insights from animal models. Schizophr Bull. 2011; 37 (3):484–492. [PubMed: 21505115]

Paus T, Keshavan M, Giedd JN. Why do many psychiatric disorders emerge during adolescence? Nat Rev Neurosci. 2008; 9 (12):947–957. [PubMed: 19002191]

Paxinos, G.; Watson, C. The Rat Brain in Stereotaxic Coordinates. Academic Press; New York: 1998.

Philpot BD, Lim JH, Brunjes PC. Activity-dependent regulation of calcium-binding proteins in the developing rat olfactory bulb. J Comp Neurol. 1997; 387 (1):12–26. [PubMed: 9331168]

Rao SG, Williams GV, Goldman-Rakic PS. Destruction and creation of spatial tuning by disinhibition: GABA(A) blockade of prefrontal cortical neurons engaged by working memory. J Neurosci. 2000; 20 (1):485–494. [PubMed: 10627624]

Rotaru DC, Barrionuevo G, Sesack SR. Mediodorsal thalamic afferents to layer III of the rat prefrontal cortex: synaptic relationships to subclasses of interneurons. J Comp Neurol. 2005; 490 (3):220–238. [PubMed: 16082676]

Schwaller B. Cytosolic Ca2+ buffers. Cold Spring Harb Perspect Biol. 2010; 2 (11):a004051. [PubMed: 20943758]

Sherwood CC, Raghanti MA, Stimpson CD, Spocter MA, Uddin M, Boddy AM, Wildman DE, Bonar CJ, Lewandowski AH, Phillips KA, Erwin JM, Hof PR. Inhibitory interneurons of the human prefrontal cortex display conserved evolution of the phenotype and related genes. Proc Biol Sci. 2010; 277 (1684):1011–1020. [PubMed: 19955152]

Solbach S, Celio MR. Ontogeny of the calcium binding protein parvalbumin in the rat nervous system. Anat Embryol (Berl). 1991; 184 (2):103–124. [PubMed: 1952098]

Spear LP. The adolescent brain and age-related behavioral manifestations. Neurosci Biobehav Rev. 2000; 24 (4):417–463. [PubMed: 10817843]

Swanson LW. A direct projection from Ammon's horn to prefrontal cortex in the rat. Brain Res. 1981; 217 (1):150–154. [PubMed: 7260612]

Tseng KY, Chambers RA, Lipska BK. The neonatal ventral hippocampal lesion as a heuristic neurodevelopmental model of schizophrenia. Behav Brain Res. 2009; 204 (2):295–305. [PubMed: 19100784]

Tseng KY, Lewis BL, Hashimoto T, Sesack SR, Kloc M, Lewis DA, O'Donnell P. A neonatal ventral hippocampal lesion causes functional deficits in adult prefrontal cortical interneurons. J Neurosci. 2008; 28 (48):12691–12699. [PubMed: 19036962]

Tseng KY, O'Donnell P. Post-pubertal emergence of prefrontal cortical up states induced by D1-NMDA co-activation. Cereb Cortex. 2005; 15 (1):49–57. [PubMed: 15217899]

Tseng KY, O'Donnell P. Dopamine modulation of prefrontal cortical interneurons changes during adolescence. Cereb Cortex. 2007; 17 (5):1235–1240. [PubMed: 16818475]

Uhlhaas PJ, Singer W. Abnormal neural oscillations and synchrony in schizophrenia. Nat Rev Neurosci. 2010; 11 (2):100–113. [PubMed: 20087360]

Uhlhaas PJ, Singer W. The development of neural synchrony and large-scale cortical networks during adolescence: relevance for the pathophysiology of schizophrenia and neurodevelopmental hypothesis. Schizophr Bull. 2011; 37 (3):514–523. [PubMed: 21505118]

Vincent SL, Pabreza L, Benes FM. Postnatal maturation of GABA-immunoreactive neurons of rat medial prefrontal cortex. J Comp Neurol. 1995; 355 (1):81–92. [PubMed: 7636016]

Volk DW, Austin MC, Pierri JN, Sampson AR, Lewis DA. Decreased glutamic acid decarboxylase67 messenger RNA expression in a subset of prefrontal cortical gamma-aminobutyric acid neurons in subjects with schizophrenia. Arch Gen Psychiatry. 2000; 57 (3):237–245. [PubMed: 10711910]

Woo TU, Whitehead RE, Melchitzky DS, Lewis DA. A subclass of prefrontal gamma-aminobutyric acid axon terminals are selectively altered in schizophrenia. Proc Natl Acad Sci U S A. 1998; 95 (9):5341–5346. [PubMed: 9560277]

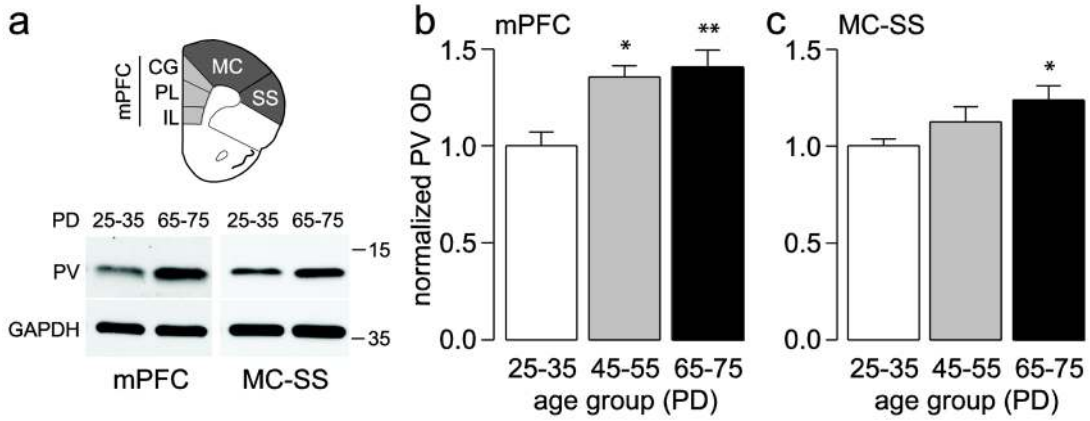

Figure 1.

(a) Diagram corresponding to the regions excised used to measure the amount of PV protein levels in the PFC. Insets below are examples of immunoblots from the medial PFC (mPFC; IL: infralimbic; PL: prelimbic; CG: cingulated) and the motor cortex-somatosensory (MC-SS) regions illustrating the age-dependent upregulation of PV protein levels observed in adults compared to juveniles. **(b,c)** Summary of PV expression (mean ± SEM) in the mPFC **(b)** and MC-SS **(c)** from juvenile (PD25–35, n=9), adolescent (PD45–55, n=5), and adult rats (PD65–75, n=9). *p<0.05, **p<0.005, Tukey *post-hoc* test after significant one-way ANOVA (mPFC main effect of age $F_{(2,20)}$=9.11, p=0.0015; MC-SS main effect of age $F_{(2,20)}$=4.32, p=0.0276)

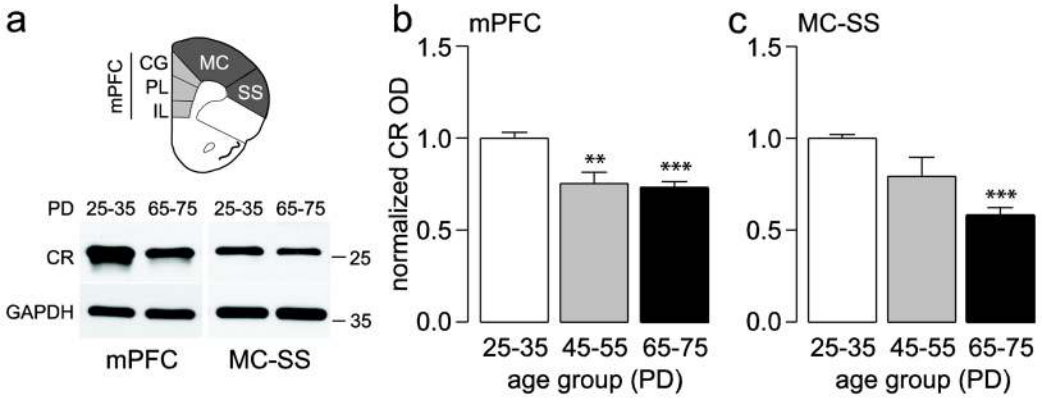

Figure 2.

(a) Diagram corresponding to the regions of the PFC excised to measure the amount of CR protein levels. Insets below are examples of immunoblots illustrating the age-dependent downregulation of CR protein levels observed in adults compared to juveniles. **(b,c)** Bar graphs summarizing the data (mean ± SEM) of CR expression in the mPFC **(b)** and MC-SS **(c)** from juvenile (PD25–35, n=9), adolescent (PD45–55, n=5), and adult rats (PD65–75, n=9). **p<0.005, ***p<0.0005, Tukey *post-hoc* test after significant one-way ANOVA (mPFC main effect of age $F_{(2,20)}$=16.61, p<0.00005; MC-SS main effect of age $F_{(2,20)}$=22.73, p<0.00005).

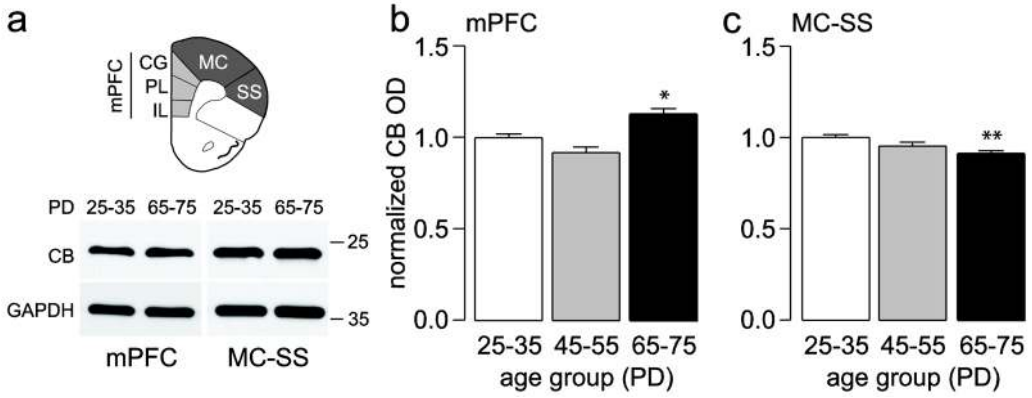

Figure 3.

(a) Diagram showing the prefrontal regions excised to measure the amount of CB protein levels. Inset below are examples of immunoblots obtained from juveniles and adults. **(b,c)** Summary of the results (mean ± SEM) from the mPFC **(b)** and MC-SS **(c)** in juvenile (PD25–35, n=9), adolescent (PD45–55, n=5), and adult rats (PD65–75, n=9). *p<0.05, **p<0.005, Tukey *post-hoc* test after significant one-way ANOVA (mPFC main effect of age $F_{(2,20)}$=12.76, p=0.00027; MC-SS main effect of age $F_{(2,20)}$=8.30, p=0.00238).

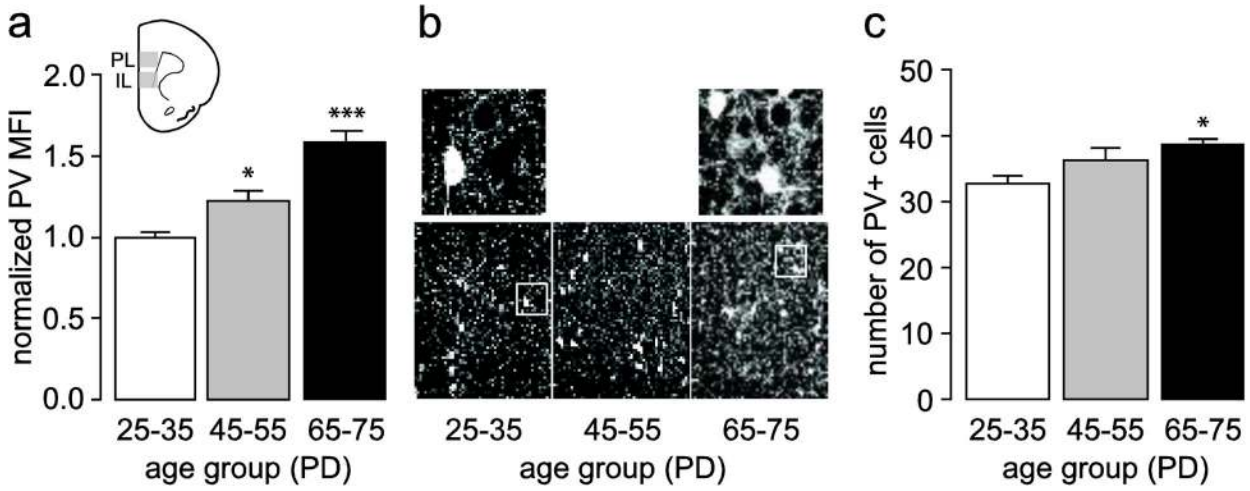

Figure 4.

(a) Measurement of mean PV fluorescence intensity in the medial PFC (IL and PL) of juvenile (PD25–35, n=8), adolescent (PD45–55, n=8), and adult (PD65–75, n=8) rats. All values (mean ± SEM) were normalized to the PD25–35 group. Similar to the immunoblots (Fig. 1), PV immunoreactivity is lowest in juveniles and increases through adolescence to adult levels (main effect of age $F_{(2,21)}$=24.12, p<0.00005, one-way ANOVA; *p<0.05, ***p<0.0005 vs. PD25–35, Tukey *post-hoc* test). **(b)** Immunofluorescence images of prefrontal PV immunoreactivity (200X of the prelimbic region) illustrating the characteristic developmental increase observed in adolescents and adults relative to juveniles. Top insets show representative details of the distinct pattern of PV-positive processes found in the juvenile and adult medial PFC. **(c)** Summary of the cell count from the same sections used in (**a)** depicting a small but significant increase in the number of PV-positive cells only in adults compared to juveniles (main effect of age $F_{(2,21)}$=4.60, p=0.02216, one-way ANOVA; *p<0.05 vs. PD25–35, Tukey *post-hoc* test).

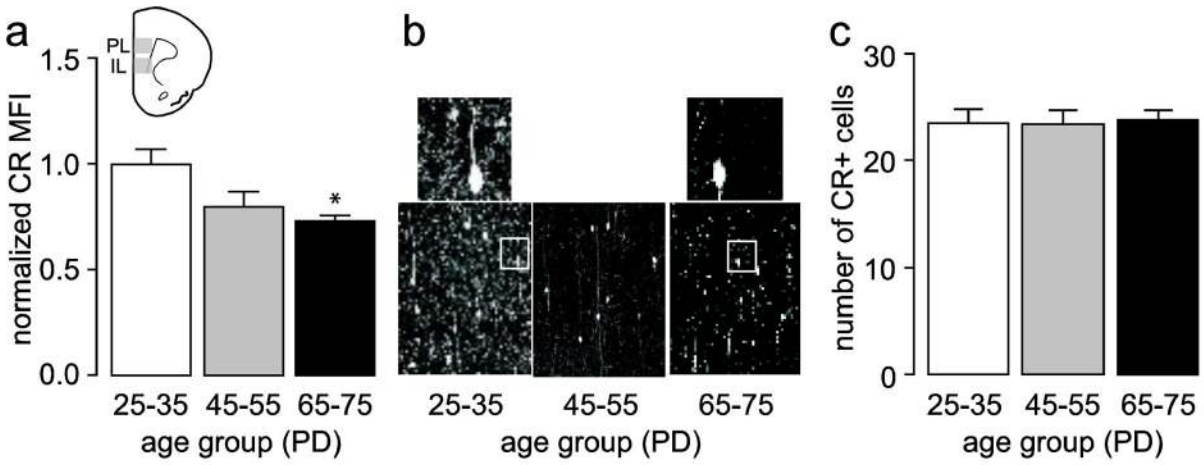

Figure 5.

(**a**) Measurement of mean CR fluorescence intensity in the medial PFC (IL and PL) of juvenile (PD25–35, n=8), adolescent (PD45–55, n=8), and adult (PD65–75, n=8) rats. All values (mean ± SEM) were normalized to the PD25–35 group average. Similar to the immunoblots (Fig. 2), CR immunoreactivity is high in juveniles and decreases in adolescent and adult animals (main effect of age $F_{(2,21)}$=5.317, p=0.01354, one-way ANOVA; *p<0.05 vs. PD25–35, Tukey *post-hoc* test). **(b)** Representative images illustrating the characteristic age-dependent decrease in CR immunoreactivity observed in the medial PFC (200X of the prelimbic region). Top insets show representative details of the distinct pattern of CR-positive processes found in the juvenile and adult medial PFC. **(c)** Summary of CR-positive cell counts in the same section used in (**a**) demonstrating no statistical differences in cell numbers across the three age groups studied.

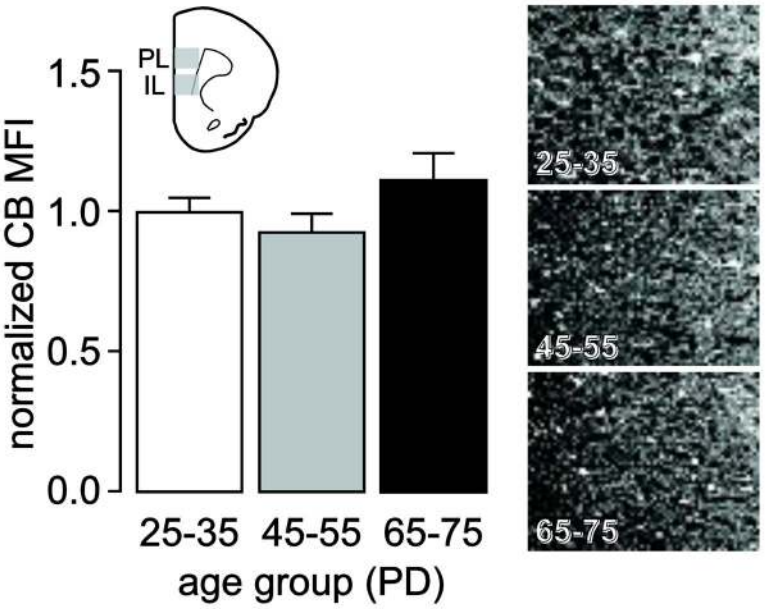

Figure 6.

Summary of mean CB fluorescence intensity analyses conducted in the medial PFC (PL and IL) of juvenile (PD25–35, n=8), adolescent (PD45–55, n=8), and adult (PD65–75, n=8) rats. All values (mean ± SEM) were normalized to the PD25–35 group average. CB immunoreactivity remained stable across the three age groups examined as revealed by a non-significant ANOVA. Top insets are representative images obtained from the medial PFC (200X of the prelimbic region) illustrating the characteristic CB immunoreactivity observed in juvenile, adolescents, and adult animals.

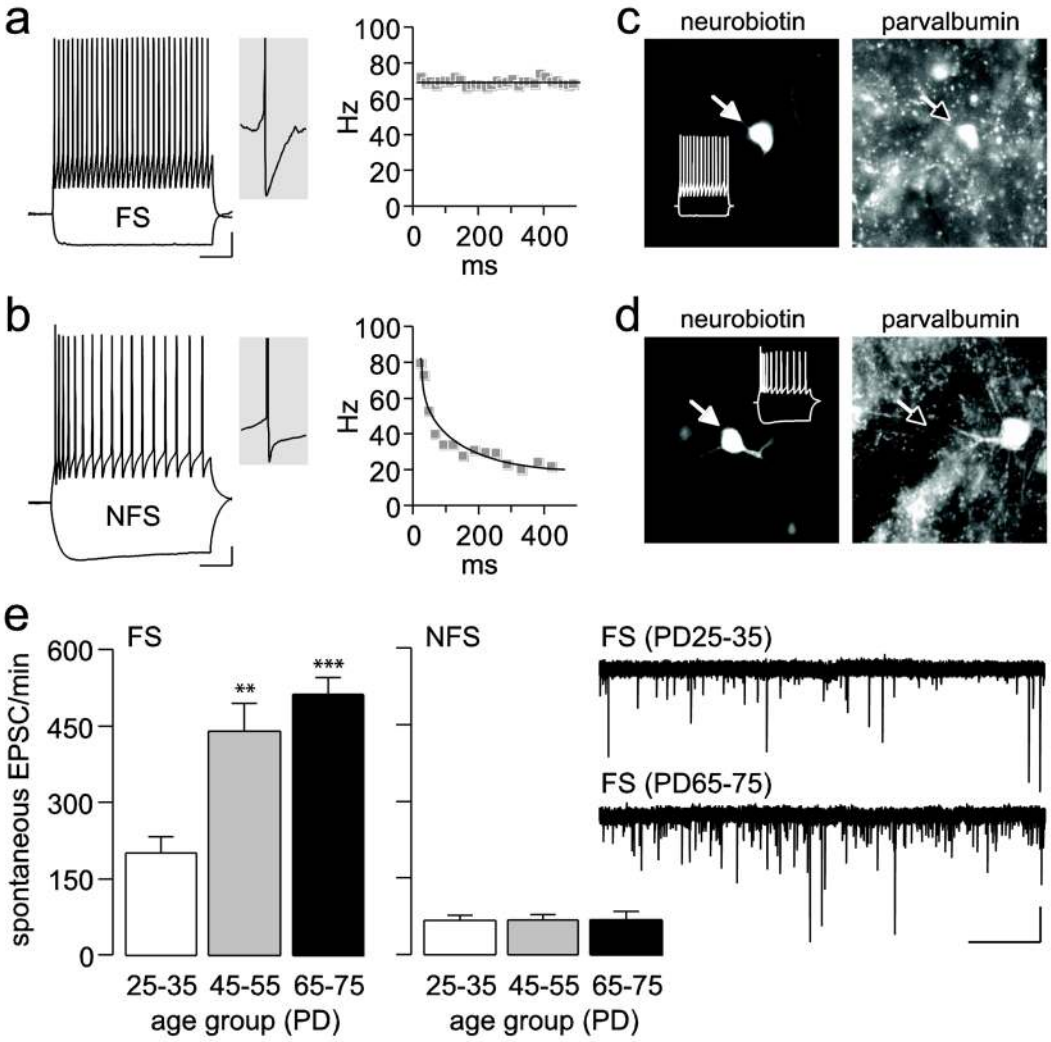

Figure 7.

(a–b) Traces illustrating the electrophysiological characteristics of prefrontal FS and NFS interneurons in response to somatic current depolarization (calibration bars: 10 mV/100 ms). FS interneurons exhibit a pronounced fast AHP (*middle panel inset*) and display a characteristic nonadapting firing response as indicated by the constant instantaneous firing rate (Hz) throughout the current pulse depolarization. In contrast, NFS interneurons show a typical spike-frequency adaptation response to somatic current depolarization and a less pronounced AHP (*middle panel inset*). **(c–d)** Examples of neurobiotin-labeled FS and NFS interneurons probed with a rabbit anti-PV. All 18 FS interneurons examined were found to be PV-positive. In contrast, none of the 16 NFS interneurons examined showed positive labeling for PV. Inset white traces show the firing pattern of the labeled neurons. **(e)** Bar graphs summarizing the cell-type specific postnatal developmental upregulation of glutamatergic synaptic transmission (i.e., number of spontaneous EPSC events per min) onto FS interneurons in the medial PFC during the periadolescent transition to adulthood (n=10 cells per age group; main effect of age $F_{(2,27)}$=15.55, p<0.00005, one-way ANOVA; **p<0.005, ***p<0.0005 vs. PD25–35, Tukey *post-hoc* test). Such developmental upregulation is lacking in NFS interneurons (n=10–11 per age group). Inset traces illustrating the periadolescent increase in the number of spontaneous EPSC events recorded from FS interneurons (calibration bars: 20 pA/3 s).

Table 1

Basic electrophysiological properties of FS and NFS interneurons in the medial PFC

	PD25–35	PD45–55	PD65–75
Fast-spiking Interneuron	n=10	n=10	n=10
resting membrane potential (mV)[#]	−65.39 ± 0.84	−67.59 ± 1.07	−68.78 ± 0.83[*]
input resistance (MΩ)	247.10 ± 15.38	207.70 ± 18.83	208.42 ± 17.23
AP width at half amplitude (ms)	0.66 ± 0.04	0.58 ± 0.03	0.58 ± 0.02
AHP amplitude (mV)[#]	20.27 ± 0.66	22.31 ± 0.64	22.62 ± 0.63[*]
Non fast-spiking Interneuron	n=10	n=11	n=10
resting membrane potential (mV)	−66.96 ± 0.71	−67.64 ± 1.14	−66.44 ± 1.20
input resistance (MΩ)	357.41 ± 28.26	307.80 ± 33.24	285.23 ± 38.28
AP width at half amplitude (ms)	1.15 ± 0.06	1.08 ± 0.07	1.08 ± 0.08
AHP amplitude (mV)	13.26 ± 0.94	13.19 ± 1.10	13.14 ± 0.79

[#] $p<0.05$ main effect of age, one-way ANOVA (resting membrane potential: $F_{(2, 27)}=3.49$; AHP amplitude: $F_{(2, 27)}=3.96$)

[*] $p<0.05$ vs. PD25–35, Tukey *post-hoc* test after significant one-way ANOVA

AP: action potential; AHP: after hyperpolarization